



Contents lists available at ScienceDirect

Physica D

journal homepage: [www.elsevier.com/locate/physd](http://www.elsevier.com/locate/physd)

## Pacer cell response to periodic Zeitgebers

D.G.M. Beersma<sup>b</sup>, H.W. Broer<sup>a</sup>, K. Efstathiou<sup>a</sup>, K.A. Gargar<sup>b</sup>, I. Hoveijn<sup>a,\*</sup>

<sup>a</sup> Johann Bernoulli Institute for Mathematics and Computer Science, The Netherlands

<sup>b</sup> Department of Chronobiology, University of Groningen, The Netherlands

### ARTICLE INFO

#### Article history:

Received 30 July 2010

Received in revised form

27 June 2011

Accepted 27 June 2011

Available online xxxx

Communicated by B. Sandstede

#### Keywords:

Circadian clock

Phase oscillator

Zeitgeber

Synchronization

Circle map

Resonance tongue

### ABSTRACT

Almost all organisms show some kind of time periodicity in their behavior. In mammals, the neurons of the suprachiasmatic nucleus form a biological clock regulating the activity–inactivity cycle of the animal. The main question is how this clock is able to entrain to the natural 24 h light–dark cycle by which it is stimulated. Such a system is usually modeled as a collection of mutually coupled two-state (active–inactive) phase oscillators with an external stimulus (Zeitgeber). In this article however, we investigate the entrainment of a single pacer cell to the ensemble of other pacer cells. Moreover the stimulus of the ensemble is taken to be periodic. The pacer cell interacts with its environment by phase delay at the end of its activity interval and phase advance at the end of its inactivity interval. We develop a mathematical model for this system, naturally leading to a circle map depending on parameters like the intrinsic period and phase delay and advance. The existence of resonance tongues in a circle map shows that an individual pacer cell is able to synchronize with the ensemble. We furthermore show how the parameters in the model can be related to biological observable quantities. Finally we give several directions of further research.

© 2011 Elsevier B.V. All rights reserved.

## 1. Introduction

### 1.1. Setting of the problem

Rhythmic behavior is present in almost all organisms. Their rhythms can be autonomous and usually they are externally stimulated. One such stimulus is the 24 h natural light–dark cycle which governs the activity–inactivity cycle of many animals and plants. The latter is the most common *Zeitgeber* or periodic stimulus, although an alternating high–low temperature cycle is another example of a *Zeitgeber*. After millions of years of evolution, many organisms exhibit periodic behavior with a period near 24 h [1], even in conditions without information on the alternation of light and darkness. How the almost-24 h *intrinsic period* of the internal rhythm synchronizes with or entrains to an external *Zeitgeber* is one of the major questions in circadian biology; see [2, 3].

In mammals, the circadian clock resides in the suprachiasmatic nucleus, a neuronal hypothalamic tissue residing just above the optic chiasm. It consists of about 10 000 interconnected neurons or pacer cells [4–7]. In [8] a model appeared for explaining circadian rhythms of the suprachiasmatic nucleus as a collection of so-called two-state phase oscillators. We now know that there are more

cell types contained in the suprachiasmatic nucleus; see [9–12]. Experiments *in vitro* with cells from the suprachiasmatic nucleus, for example in [10,13], reveal that not all cells show periodic activity. It is not completely clear whether or how these cells contribute to entrainment. Therefore, in this article, we consider a set of similar, but not equal, two-state pacer cells that can be modeled as two-state phase oscillators. Moreover we restrict to an investigation of entrainment of a single pacer cell to the ensemble of other pacer cells. For simplicity we assume that the signal provided by the other cells is periodic. The mathematical work is inspired by earlier computational simulations of the interacting network, which revealed that an ensemble of interacting pacers has characteristics that are not present at the level of individual cells. In particular, the ensemble can adjust the period of its rhythm to the period of the signal to which it is exposed. The ensemble continues to oscillate with about that period for a while, even if the synchronizing signal is turned off. This phenomenon, which shows robustness of the biological clock against perturbations of the entraining signal, is functionally relevant even under normal 24 h routines. The current investigation shows how individual cells synchronize to the ensemble. The biological clock as a whole generates a smooth and rather sinusoidal signal, whereas single pacer cells are known to generate electrical activity rhythms that can hardly be considered continuous. Long intervals of silence are followed by relatively short intervals in which action potentials are generated. Although the discharge rate in these intervals varies, we simplify this in our model by assuming that cells demonstrate

\* Corresponding author.

E-mail addresses: [I.Hoveijn@rug.nl](mailto:I.Hoveijn@rug.nl), [ihoveijn@home.nl](mailto:ihoveijn@home.nl) (I. Hoveijn).

two states: silence versus activity. Doing this, the dynamics of the behavior of each cell is characterized by the timing of the state transitions. The basis for our model of a single pacer cell is given in [14,8] where the state of a pacer cell is determined by the phase in its activity–inactivity cycle. Furthermore an external stimulus, depending on its timing, has the effect of delaying the phase of the oscillator in the active state and advancing the phase in the inactive state. This model is used to explain the observation that the activity–inactivity cycle of an organism closely follows the period of a Zeitgeber like the 24 h light–dark cycle. Further details of the model will be presented in Section 2.

The translation into a mathematical model closely follows the biological model just described. The result is a system of coupled oscillators with an external forcing. Despite certain results, notably [15], the mathematical analysis of such systems is notoriously hard. Therefore, in this article, we analyze a simpler system, namely a single pacer cell subject to the net stimulus of all other pacer cells and the external Zeitgeber. In this system the singled out pacer cell does not stimulate the others: so for simplicity we assume asymmetric coupling. In physics this is called the mean field approach. For the single pacer cell the sum of all stimuli is now the Zeitgeber. The latter can be a periodic, quasi-periodic or even more general function of time. But in this article we restrict to a (non-constant) periodic Zeitgeber where the period is an average or prevailing period in the natural light and dark cycle or in the collective behavior of pacer cells in the environment. Translating the biological model for a single pacer cell with a periodic Zeitgeber into a mathematical model naturally leads to a dynamical system consisting of a circle map. In future work we will analyze more general Zeitgebers and systems with more symmetric coupling.

In the literature there exist several models for biological clocks. A common aspect of these models is that the biological clock is considered as a collection of coupled oscillators. The assumptions about the oscillators are the most variant part. A class of models based on biochemical reactions of gene expression and products thereof in neurons take the Goodwin oscillator (see [16,17] and references therein) as a starting point. The original model [18] leads to a three-dimensional system of ordinary differential equations. The system contains parameters describing the reaction kinematics and for a large set of parameter values there exists a stable periodic orbit. For models including many more biochemical reactions see [19,20]. It follows from fairly general arguments [21] that every periodically forced oscillator will show tongue shaped regions of stability in the parameter plane of period versus forcing strength. This phenomenon is inevitably observed for the Goodwin oscillator. Moreover, there is numerical evidence (see for example [17]) of synchronization in a large collection of Goodwin oscillators. At the other end of the spectrum we find models that are based on observed responses of living organisms to external stimuli in general; see [22]. Our model, using a phase oscillator, fits into this class by following [23] and in particular [14] for light and dark stimuli. Here the assumption is that the observed response of the organism is a reflection of the response of the individual neurons, although we keep in mind that a collection of interacting pacer cells may also show different behavior. The use of phase oscillators to model biological periodic phenomena dates back to at least 1967 [24]; see [25] for an overview. In between these bottom-up and top-down approaches there are several other models using oscillatory systems. However, these are not always based on an underlying biological model, examples including the periodically kicked oscillator in [26] and the van der Pol oscillator in [27]. New in our approach is the combination of a two-state phase oscillator and the interaction with the Zeitgeber through phase delay at the end of the activity interval and phase advance at the end of the inactivity interval. Also new is the relation of the

four parameters in the model (see Sections 2 and 3), via a circle map with observable biological quantities, for example the range of entrainment, and entrainment boundaries depending on the phase delay and advance.

### 1.2. The main questions

Thus we study a model of a single pacer cell, stimulated by its environment but not contributing to the collective behavior. For such a situation the main questions that we wish to address are:

1. Can a single pacer cell synchronize with or entrain to a periodic Zeitgeber?
2. If so, how does this depend on properties of the pacer cell?

To answer these questions we translate the biological model into a mathematical model, in our case a dynamical system. In fact, it will turn out that the biological model leads to a circle map. This map depends on the parameters characterizing the pacer cell. Typical dynamics of a circle map most relevant in view of the questions above are dynamics of fixed points and dynamics of periodic points. Fixed points correspond to *entrainment* of the pacer cell which means that the sequence of onset times of the activity interval has the same period as the Zeitgeber. Periodic points correspond to *synchronization* meaning that there are an integer number  $p$  of different times of onset of the activity interval during another integer number  $q$  of periods of the Zeitgeber. Such points are called  $p : q$  periodic points. In this vocabulary fixed points are  $1 : 1$  periodic points; in other words entrainment is a special kind of synchronization. Then the questions for the single pacer cell are translated into the following questions for the mathematical model.

1. Do stable fixed or periodic points exist for the map on the circle?
2. If so, for which domain in parameter space?

The first question can be answered affirmatively by the general theory of circle maps. To answer the second question we need to know more about the details of the circle map, and in particular how it depends on the parameters characterizing the pacer cell.

### 1.3. A summary of the results

The analysis of the mathematical model for a single pacer cell shows that synchronization occurs for certain values of the parameters. Indeed, several phenomena of circadian behavior can be explained by our model. First of all there is a *range of entrainment* allowing pacer cells with shorter and longer intrinsic periods to entrain to the Zeitgeber. However, depending on the values of the delay and advance parameters (see Section 2 for details), this range of entrainment favors either longer or shorter intrinsic periods. Similarly there are *ranges of synchronization* where the pacer cell shows for example multiple activity intervals during one period of the Zeitgeber; see Fig. 6. This means that only for a finite interval of values of the intrinsic period, synchronization is possible, a phenomenon which is confirmed by biological experiments and observations; see [28,2,29,25,30–32,23,33–37]. Outside the ranges of synchronization the model predicts quasi-periodic behavior of the pacer cell, which is related to the biological phenomenon called relative coordination. Furthermore, the model predicts that the onset of an activity interval increases with the intrinsic period of the pacer cell, which has been observed for many organisms; see [29,28,38,37]. Thus in our model, the values of the parameters can be related to biologically observable phenomena.

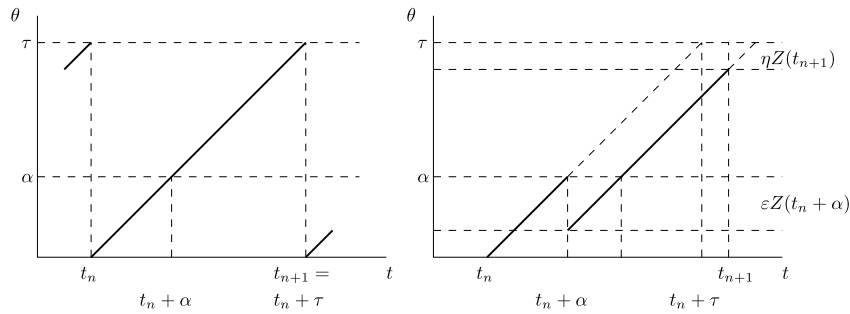


**Fig. 1.** The phase  $\theta$  as a function of  $t$  without (left) and with (right) the Zeitgeber. Suppose the phase  $\theta$  is 0 at time  $t_n$ ; then the state of the cell is active for  $0 \leq \theta < \alpha$  and inactive for  $\alpha \leq \theta < \tau$ . Without the Zeitgeber (left figure) this corresponds to the time intervals  $[t_n, t_n + \alpha)$  and  $[t_n + \alpha, t_n + \tau)$ . In the presence of a Zeitgeber the cell is active in the time interval  $[t_n, t_n + \alpha + \varepsilon Z(t_n + \alpha))$  and inactive in the time interval  $[t_n + \alpha + \varepsilon Z(t_n + \alpha), t_{n+1})$ , where  $t_{n+1}$  is defined implicitly; see the text.

## 2. The biological model

Our biological model is derived from [14]. Each pacer cell is considered as a two-state phase oscillator, where the phase is determined by a single variable  $\theta$  taking values in  $[0, \tau]$ . This phase is the resultant of many biochemical processes. In an isolated pacer cell the phase increases in time with speed 1 until it reaches a value  $\tau$ ; then it jumps to zero and starts to increase again. The two states of the pacer cell are characterized as follows. If the phase is between zero and a value  $\alpha < \tau$ , the cell is in the *active* state, and for the phase between  $\alpha$  and  $\tau$ , the cell is in the *inactive* state. Thus an isolated pacer cell shows a periodic activity–inactivity cycle with period  $\tau$ . We call  $\alpha$  the length of the *intrinsic activity interval*, and  $\tau$  is called the *intrinsic period* of the pacer cell. The values of  $\alpha$  and  $\tau$  are properties of the individual cell.

A pacer cell responds to external stimuli. In our model the response depends on the state of the cell. In the active state, an external stimulus delays the phase and so the activity interval is prolonged. Suppose that at  $t = t_n$  the phase is zero. When the cell is stimulated by a Zeitgeber  $Z$ , it remains active until time  $t_n + \alpha + \varepsilon Z$ , where  $\varepsilon$  is a small cell dependent parameter. We incorporate this *phase delay* into the model by delaying the phase once by an amount of  $\varepsilon Z$  at time  $t_n + \alpha$ , so instantly  $\theta$  becomes  $\theta - \varepsilon Z$ . On the other hand, during the inactive state, an external stimulus advances the phase and as a consequence the inactivity interval is shortened. If at time  $t = t_{n+1}$  the phase of the cell is below  $\tau$  by an amount  $\eta Z$ , and so  $\theta + \eta Z = \tau$ , the cell becomes active again; here  $\eta$  is another small cell dependent parameter. Thus there is a *phase advance* of  $\theta$  by an amount  $\eta Z$  at time  $t_{n+1}$ ; that is, instantly  $\theta$  becomes  $\theta + \eta Z$ . Since the latter is equal to  $\tau$ , the phase jumps to zero, and the cell is again in the active state; see Fig. 1.

Our long-term goal is to model a collection of interacting pacer cells subject to stimulation by a Zeitgeber, the *external stimulus*. In our model the interaction of the pacer cells is by stimulation via the average of the activity of other pacer cells; let us call this an *internal stimulus*. The average may depend on spatial structure of the collection of pacer cells, but for the moment we assume that there is none. Thus the total stimulus that a pacer cell in a collection experiences is a (weighted) sum of the internal and external stimuli. However, when we translate our biological model into a mathematical model we are confronted with the fact that a mathematical analysis of coupled oscillators is difficult. Therefore we make the following simplification, which is known in physics as the mean field approach. In a collection of pacer cells we single out one. This pacer cell experiences a stimulus which is the sum of internal and external stimuli. For the pacer cell this sum of stimuli will now be the Zeitgeber. However, the pacer cell singled out does not contribute to the sum of stimuli.

In principle the Zeitgeber  $Z$  for the pacer cell singled out can be any function of time. Here we will take it periodic, where

the period is for example an average of the observed periods of the collection of pacer cells or an average period of an external stimulus like the daily light and dark cycle. But we may also take a much longer period to model seasonal effects. Since pacer cells may have different values of  $\varepsilon, \eta, \alpha$  and  $\tau$  we are especially interested in the domain in parameter space where synchronization occurs.

## 3. The mathematical model

The system described in Section 2 has a state which evolves in time. This calls for a *dynamical systems* approach; as a general reference see [39]. In order to adopt such an approach we have to identify a *state space* and an *evolution law*. This means that we should find one or more quantities describing the state of the system, and then find an evolution law that uniquely defines a future state once an initial state is given. Here we restrict to *deterministic dynamical systems*; that is, we do not include noise or some other kinds of random fluctuations. It will turn out that we can define a discrete dynamical system on the circle. Using this model we are able to answer some of the questions in Section 1 for a single pacer cell with a Zeitgeber.

*An isolated pacer cell.* The model that we build is based on the phase  $\theta$  of the cell. First we consider the cell as a ‘free running’ oscillator, depending on the two parameters  $\alpha$  and  $\tau$ . Later on we also include a periodic Zeitgeber with two additional parameters  $\varepsilon$  and  $\eta$  governing the strength of the forcing.

Let  $\theta : \mathbb{R} \rightarrow [0, \tau)$  be the phase of the cell given by

$$\theta(t) = \begin{cases} t - t_n, & \text{for } t \in [t_n, t_{n+1}) \\ 0, & \text{for } t = t_{n+1}, \end{cases}$$

where  $\tau$  is the maximal value of  $\theta$ . When  $\theta$  reaches the value  $\alpha$ , with  $0 < \alpha < \tau$ , the cell undergoes the transition from active to inactive. Suppose at  $t = t_n$  the phase  $\theta$  is zero. The phase increases with speed 1 until it reaches the maximal value  $\tau$ ; then  $\theta$  instantly becomes zero again. This happens at time  $t = t_{n+1} = t_n + \tau$ . Thus the period of the ‘free running’ oscillator is  $\tau$ . The transition times are  $t_n = t_0 + n\tau$  and  $t_n + \alpha$  where the cell state changes from inactive to active and from active to inactive respectively; see Fig. 1.

We will use the transition times  $t_n$  in phase space  $\mathbb{R}$  to define a dynamical system whose evolution takes  $t_n$  into  $t_{n+1}$ . Without the Zeitgeber we have a sequence  $t_n = t_0 + n\tau$  as described above depending on the parameters  $\alpha$  (although trivially) and  $\tau$ . Next we include a Zeitgeber.

*A single pacer cell with a periodic Zeitgeber.* To model a non-isolated pacer cell in a collection of other pacer cells with or without an external stimulus, we consider a single pacer cell with a Zeitgeber  $Z$  which is a function of time only. First we define the Zeitgeber  $Z$  which is a function of time only. First we define the Zeitgeber  $Z$  which is a function of time only. Though non-essential, it is convenient to scale time such that the period becomes 1 and scale the Zeitgeber such that it takes values in  $[0, 1]$ .

**Definition 1.** The positive function  $Z : \mathbb{R} \rightarrow [0, 1]$  satisfies the following:

- (i)  $Z$  is differentiable,
- (ii)  $Z$  is periodic with period 1.

In the presence of a Zeitgeber the phase  $\theta$  again increases with speed 1, starting at  $\theta = 0$  at  $t = t_n$ , but when  $\theta$  reaches the value  $\alpha$  it instantly drops back by an amount of  $\varepsilon Z(t_n + \alpha)$ . Then it again increases with speed 1 until it reaches a value at  $t = t_{n+1}$  such that  $\theta(t_{n+1}) + \eta Z(t_{n+1}) = \tau$ . Note that  $t_{n+1}$  is implicitly defined. Thus the phase  $\theta$  of the cell is given by

$$\theta(t) = \begin{cases} t - t_n, & \text{for } t \in [t_n, t_n + \alpha) \\ t - t_n - \varepsilon Z(t_n + \alpha) & \text{for } t \in [t_n + \alpha, t_{n+1}) \\ 0, & \text{for } t = t_{n+1}. \end{cases} \quad (1)$$

Besides the parameters  $\alpha$  and  $\tau$  we now also have  $\varepsilon$  and  $\eta$ . The latter two give the ‘strength’ of the Zeitgeber. In order that the model be consistent we impose the following conditions on the parameters:

$$0 < \alpha < \tau, \quad \varepsilon \geq 0, \quad \eta \geq 0, \quad \alpha - \varepsilon > 0, \quad \alpha - \varepsilon + \eta < \tau,$$

so that  $\theta$  remains between 0 and  $\tau$ .

*The dynamical system.* The state of the dynamical system that we define is the transition time  $t_n$  rather than the phase  $\theta$ . Indeed solving the equation

$$\theta(t) + \eta Z(t) = \tau \quad \text{or equivalently } t - t_n - \varepsilon Z(t_n + \alpha) + \eta Z(t) = \tau \quad (2)$$

for  $t$ , under conditions to be specified later, yields a unique solution  $t = t_{n+1}$  once  $t_n$  is given. Thus we may write  $t_{n+1} = F_\mu(t_n)$  for a map  $F_\mu : \mathbb{R} \rightarrow \mathbb{R}$  depending on parameters  $\mu = (\varepsilon, \eta, \alpha, \tau)$ . However, it turns out that  $F_\mu$  has the property  $F_\mu(t+1) = F_\mu(t) + 1$ , so  $F_\mu$  is the lift of a circle map  $f_\mu : S^1 \rightarrow S^1$ . This means that we now have a dynamical system with phase space the circle  $S^1$  and evolution law  $f_\mu$ . Conceptually it is easier to work with the circle map  $f_\mu$  but for actual computations we usually prefer the lift  $F_\mu$ . Let us summarize the result in the following proposition; for a proof see the Appendix.

**Proposition 2 (Circle Map and Lift).** Let  $Z$  be as in Definition 1 and define the function  $U_\varepsilon : \mathbb{R} \rightarrow \mathbb{R}$  as  $U_\varepsilon(t) = t + \varepsilon Z(t)$ . Then the map  $F_\mu : \mathbb{R} \rightarrow \mathbb{R}$  with

$$F_\mu(t) = U_\eta^{-1}(U_\varepsilon(t + \alpha) - \alpha + \tau) \quad (3)$$

defines a parameter dependent differentiable dynamical system, provided that  $U_\eta$  is invertible. The parameters are  $\mu = (\varepsilon, \eta, \alpha, \tau)$ . Furthermore,  $F_\mu$  is the lift of a circle map  $f_\mu : S^1 \rightarrow S^1$  of degree 1, given by

$$f_\mu(t) = U_\eta^{-1}(U_\varepsilon(t + \alpha) - \alpha + \tau) \bmod 1. \quad (4)$$

A circle map is a one-dimensional map just like an interval map. The dynamics of the two have much in common; this feature is most prominent when the circle map is studied via a lift. However, because the circle is different from the interval, there are also differences in dynamical behavior. For example non-degenerate fixed points of a circle map come in pairs. See Fig. 2.

We now make a further distinction between two cases, namely whether  $f_\mu$  is invertible (a diffeomorphism) or not (an endomorphism). The difference between these cases is not only in dynamical behavior but also because the second case has far richer bifurcation scenarios. Essentially it boils down to both  $\varepsilon$  and  $\eta$  being ‘sufficiently small’ or one of them not meeting this criterion. However, there is *a priori* no reason to assume that either of them is small.

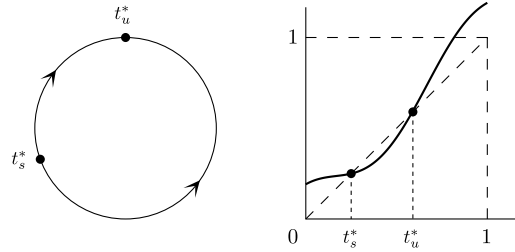


**Fig. 2.** Phase portrait of the circle map  $f_\mu$  and graph of the lift  $F_\mu$ .  $f_\mu$  has two fixed points indicated by bullets. One is stable; the other is unstable, according to the arrows. The lift  $F_\mu$  is a map on the interval  $[0, 1]$  with  $F_\mu(1) = F_\mu(0) + 1$ ; drawn is  $F_\mu - 1$ .  $t_s^*$  (stable) and  $t_u^*$  (unstable) satisfy  $F_\mu(t) = t + 1$ . The Zeitgeber in this example is  $Z(t) = \frac{1}{2}(1 + \sin(2\pi t))$ .

- (a)  **$F_\mu$  is the lift of a circle diffeomorphism.** In this case  $F_\mu$  is differentiable and  $F_\mu^{-1}$  exists and is also differentiable. Both  $U_\eta$  and  $U_\varepsilon$  have to be invertible, which in turn means that  $\varepsilon$  and  $\eta$  must be small enough; in particular,  $1 + \varepsilon Z'(t) > 0$  and  $1 + \eta Z'(t) > 0$  for all  $t$ .
- (b)  **$F_\mu$  is the lift of a circle endomorphism.** In this case  $F_\mu$  is again differentiable but  $F_\mu^{-1}$  does not necessarily exist. Now only  $U_\eta$  has to be invertible, which means that only  $\eta$  has to be small enough.

**Remark 1.** Here  $\varepsilon$  ‘small enough’ means that  $U_\varepsilon$  is invertible, for which we need that  $U_\varepsilon' > 0$ . This depends on the specific form of the Zeitgeber. For the standard Zeitgeber  $Z(t) = \frac{1}{2}(1 + \sin(2\pi t))$ , small enough means that  $\varepsilon < \frac{1}{\pi}$ . Thus the circle map  $f_\mu$  is a diffeomorphism if both  $\varepsilon$  and  $\eta$  are smaller than  $\frac{1}{\pi}$ . The standard Zeitgeber has no biological meaning; we only use it as an illustration. Since every 1-periodic function has a Fourier series containing sine and cosine terms, the standard Zeitgeber can be regarded as the simplest non-trivial example of such a function. □

**Remark 2.** If  $\eta$  is not small, but  $\varepsilon$  is small enough that  $U_\varepsilon$  is invertible,  $F_\mu^{-1}$  is the lift of a circle endomorphism, but  $F_\mu$  is multi-valued. This case is similar to case b with the roles of  $F_\mu$  and  $F_\mu^{-1}$  interchanged. However in the dynamical system defined with  $F_\mu^{-1}$ , time is running backwards, so it describes the past rather than the future. Mathematically this is not a problem, but the biological interpretation could be problematic. One could force  $F_\mu$  to be single-valued by choosing the smallest solution for  $t = t_{n+1}$  of Eq. (2). Then  $F_\mu$  again defines a dynamical system, though a discontinuous one. □

**Remark 3.** If both  $\varepsilon$  and  $\eta$  are not small,  $F_\mu$  and  $F_\mu^{-1}$  are multi-valued. In this case we do not have a well-defined dynamical system at all. But a construction similar to that in the previous remark can be applied to define a possibly discontinuous dynamical system. □

**4. Analysis of the mathematical model**

Here we restrict ourselves to the case where  $F_\mu$  in Proposition 2 is the lift of a circle diffeomorphism  $f_\mu$ . In that case we can use the rotation number which tells us how much on average an initial point is rotated along the circle by  $f_\mu$ . It is a powerful tool in determining whether  $f_\mu$  has fixed points or periodic points. The existence of such points and their dependence on the parameters  $\mu$  is the main topic of this section. Stable fixed or periodic points are the most relevant for our model and we will see how they lose stability at certain bifurcations. For background on circle maps and further references to the literature see [21,39–41].

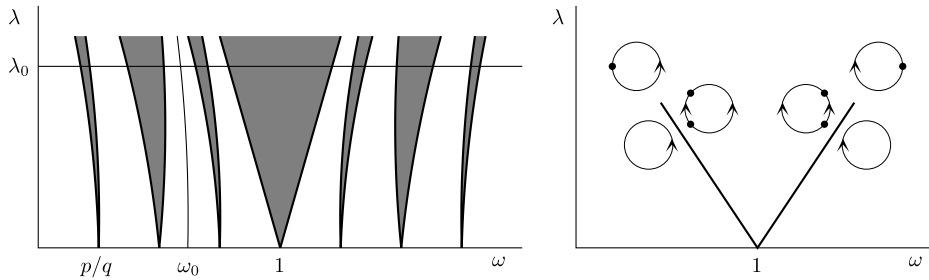


**Fig. 3.** Left: schematic picture of tongues and hairs, the main tongue emanating at 1, a  $p : q$  tongue at  $p/q$  and a hair at  $\omega_0$ , on the  $\omega$ -axis for the Arnol'd map  $A_{\omega,\lambda}$ . Right: schematic phase portraits of the same family near and on the boundary of the main tongue. The rotation number as a function of  $\omega$  for a fixed value  $\lambda = \lambda_0$  is shown in Fig. 4.

4.1. Special cases related to the Arnol'd map

We begin with an example, namely two special cases where  $F_\mu$  can be related to the lift of the Arnol'd or standard circle map  $A_{\omega,\lambda}$ . Here we make a special choice for the Zeitgeber  $Z$ , namely  $Z(t) = \frac{1}{2}(1 + \sin(2\pi t))$ . The rotation number of the Arnol'd map, depending on the parameters  $\omega$  and  $\lambda$ , is well studied, so we have quite some information on fixed and periodic points. The (lift of the) Arnol'd map is defined as

$$A_{\omega,\lambda}(t) = t + \omega + \lambda \sin(2\pi t),$$

for  $t \in \mathbb{R}$  and parameters  $\lambda, \omega \in \mathbb{R}$ . In Fig. 3 we indicate the regions in the  $(\omega, \lambda)$ -plane where the rotation number of  $A_{\omega,\lambda}$  is constant. These regions are called *tongues* and the general theory of circle diffeomorphisms tells us that for parameter values inside the tongues the map has stable fixed or periodic points. On the tongue boundaries we have saddle-node bifurcations of fixed points in the main tongue or periodic points in the other tongues; see Fig. 3.

Recall that the lift of our circle map  $f_\mu$  is given by  $F_\mu(t) = U_\eta^{-1}(U_\varepsilon(t + \alpha) - \alpha + \tau)$ , where  $U_\varepsilon(t) = t + \varepsilon Z(t)$  and  $Z$  is the periodic forcing. For a special choice of  $Z$  and parameters  $\mu$ ,  $F_\mu$  is transformed into the Arnol'd map by a change of coordinates. We summarize this in the following lemma.

**Lemma 3** (Conjugation to the Arnol'd Map). *Let the periodic Zeitgeber  $Z$  be given by  $Z(t) = \frac{1}{2}(1 + \sin(2\pi t))$ ; then:*

1. the map  $F_{(\varepsilon,0,\alpha,\tau)}$  is conjugate to the Arnol'd map  $A_{\tau+\frac{1}{2}\varepsilon, \frac{1}{2}\varepsilon}$ , where the conjugation is a rigid translation over  $\alpha$ ,
2. the map  $F_{(0,\eta,\alpha,\tau)}^{-1}$  is equal to the Arnol'd map  $A_{-\tau+\frac{1}{2}\eta, \frac{1}{2}\eta}$ .

Using  $F^{-1}$  in the second part of the lemma may seem unnatural in the present context, but if  $\rho$  is the rotation number of  $F^{-1}$ , then  $1 - \rho$  is the rotation number of  $F$ . Therefore the second part yields information about the rotation number of  $F_{(0,\eta,\alpha,\tau)}$ . Note that the parameter transformation from parameters of  $F$  to those of  $A$  does not involve  $\alpha$ . Thus  $\alpha$  does not play a role in the bifurcation analysis of these two special cases. The proof of the lemma is straightforward and therefore omitted.

To analyze these two special cases it suffices to consider the Arnol'd map  $A_{\omega,\lambda}$ . Let us summarize the properties of the latter. If  $\lambda = 0$ , the map reduces to a rigid rotation  $A_{\omega,0} = R_\omega$  and therefore the rotation number is  $\rho(A_{\omega,0}) = \rho(R_\omega) = \omega$ . This is a degenerate situation. But for  $\lambda \neq 0$  the map is no longer degenerate. Let us first fix  $\omega = \omega_0$  and  $\lambda = \lambda_0 \neq 0$  such that  $A_{\omega_0,\lambda_0}$  has a rational rotation number  $\frac{p}{q}$ . Then  $A_{\omega_0,\lambda_0}$  has  $q$ -periodic points. If these points are hyperbolic then there is an open neighborhood of  $(\omega_0, \lambda_0)$  in the parameter plane such that for all  $(\omega, \lambda)$  in this neighborhood,  $A_{\omega,\lambda}$  has rotation number  $\frac{p}{q}$ .

Let us now consider the line  $L_{\lambda_0} = \{(\omega, \lambda_0) \mid \lambda_0 \neq 0, \omega \in [\frac{1}{2}, \frac{3}{2}]\}$  in the parameter plane of the Arnol'd circle map. From the arguments above it follows that this line segment contains

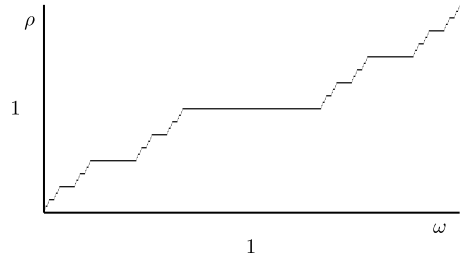


**Fig. 4.** Devil's staircase: the graph of the rotation number  $\rho$  as a function of  $\omega$  for the Arnol'd map at a fixed value  $\lambda = \lambda_0$ . In the main tongue the rotation number is equal to 1. Also see Fig. 3.

open intervals on which the rotation number of the map equals  $\frac{p}{q}$ . These intervals have to shrink to points when  $\lambda_0$  tends to zero, because the rotation number of  $A_{\omega,0}$  equals  $\omega$ . When we consider the rotation number on the line segment  $L_{\lambda_0}$  as a function of  $\omega$ , its graph (see Fig. 4) is a so-called *devil's staircase*; see [40,41] for a definition. A further analysis shows that there are saddle-node bifurcations of  $q$ -periodic points on the boundary of the intervals in  $L_{\lambda_0}$ ; see [42]. Since the map  $A_{\omega,\lambda}$  is differentiable in the parameters  $\omega$  and  $\lambda$  there are differentiable pairs of saddle-node curves in the  $(\omega, \lambda)$ -parameter plane emanating from rational points on the line segment  $L_0$ . This forms the structure of *tongues* in the parameter plane; see Fig. 3. The tongues where the rotation number is  $\frac{p}{q}$  are called  $p : q$ -tongues and the tongue where the rotation number is 1 (or 0) is called the *main tongue*.

A rational rotation number  $\frac{p}{q}$  for the map  $A_{\omega,\lambda}$  is constant on closed intervals on the line segment  $L_{\lambda_0}$ . But the complement of the union of these closed intervals in  $L_{\lambda_0}$  is not empty; it contains points where the rotation number is irrational. Again when  $\lambda_0$  tends to zero there are smooth curves with sufficiently irrational rotation number ending in irrational points of  $L_0$ . These curves are sometimes called *hairs*. The  $(\omega, \lambda)$ -parameter plane of the Arnol'd circle map consists mainly of *tongues* and *hairs*; see Fig. 3. The tongues and hairs fill a relatively large region in the parameter plane; when we take a point  $(\omega, \lambda)$  at random, there is a positive probability that it belongs to a tongue, but there is a positive probability as well that it lies on a hair.

4.2. A standard form for the circle diffeomorphism  $f_\mu$

The purpose of this section is to show that there is a standard form for every circle diffeomorphism. The Arnol'd map for example already is in this form. Identifying the standard form for the map  $f_\mu$  allows us to conclude that it has a tongues-and-hairs structure in a certain parameter plane for every 1-periodic Zeitgeber. Thus the standard form mainly serves a theoretical purpose; for actual computations it is far more advantageous to use the expression in Eq. (3) for the lift of  $f_\mu$ .

**Theorem 4** below shows that every lift  $C$  of a differentiable circle map of degree 1 can be written in the following form:

$$C(t) = t + P(t),$$

where  $P$  is a 1-periodic function. We assume that  $P$  is non-zero and non-constant. The Fourier coefficients of  $P$  may be considered as parameters. Let  $\langle P \rangle$  denote the average of  $P$ . Set  $\omega = \langle P \rangle$  and  $P_0 = P - \langle P \rangle$ . Then  $\omega$  is the constant term of the Fourier series of  $P$  and  $P_0$  has zero average. Consequently  $\lambda = \max_{[0,1]} |P_0|$  is non-zero and we may set  $P_{01} = \frac{1}{\lambda} P_0$ . Finally we may write

$$C_{\omega,\lambda}(t) = t + \omega + \lambda P_{01}(t). \tag{5}$$

If we now interpret  $\omega$  and  $\lambda$  as parameters, then there is a tongues-and-hairs structure in the  $(\omega, \lambda)$ -plane. Note that we recover the Arnol'd map by setting  $P_{01}(t) = \sin(2\pi t)$ . In the more general family of Eq. (5) the tongues may have a richer structure than those of the Arnol'd map. For example there may be more saddle-node curves inside a tongue, as we will see in the next section. For a detailed description of such phenomena see [43].

Recall that  $F_\mu(t) = U_\eta^{-1}(U_\varepsilon(t + \alpha) - \alpha + \tau)$ , where  $U_\varepsilon(t) = t + \varepsilon Z(t)$  is a lift of the circle diffeomorphism  $f_\mu$ . First we give a standard form for the map  $F_\mu$ .

**Theorem 4 (Standard Form).** *Suppose that  $\eta$  is small enough that  $U_\eta^{-1}$  exists. Let  $\nu = (\sigma, \beta, \alpha, \tau)$  be new coordinates in parameter space with  $\varepsilon = \sigma \cos \beta$  and  $\eta = \sigma \sin \beta$ . Then there are smooth functions  $\omega$  and  $\lambda$  of the parameters  $\nu$  with  $\omega(\nu)|_{\sigma=0} = \tau$ ,  $\lambda(\nu) = \sigma$  and a 1-periodic smooth function  $R_\nu$  with zero average, smoothly depending on parameters  $\nu$ , such that*

$$F_{\mu(\nu)}(t) = t + \omega(\nu) + \lambda(\nu)R_\nu(t).$$

The theorem shows that after a transformation of parameters,  $F_\mu$  takes the standard form of a circle map. In particular we have the result that there is a tongues-and-hairs structure in the  $(\tau, \sigma)$ -plane, for each value of  $\beta \in [0, \frac{\pi}{2})$  and each value of  $\alpha \in [0, \tau)$ .

The function  $R$  depends on the Zeitgeber  $Z$ , but also on all parameters  $\nu$ . The latter will appear in the coefficients of the Fourier series of  $R$ .

**Remark 4.** Setting  $\eta = 0$  in  $\mu = (\varepsilon, \eta, \alpha, \tau)$  corresponds to setting  $\beta = 0$  in  $\nu = (\sigma, \beta, \alpha, \tau)$ . Let  $\langle Z \rangle = \int_0^1 Z(t) dt$  be the average of  $Z$ ; then we have

$$\begin{aligned} F_{(\varepsilon,0,\alpha,\tau)} &= t + \tau + \varepsilon Z(t + \alpha) \\ &= t + \tau + \varepsilon \langle Z \rangle + \varepsilon(Z(t + \alpha) - \langle Z \rangle). \end{aligned}$$

If we also take  $Z(t) = \frac{1}{2}(1 + \sin(2\pi t))$  we recover the result of Lemma 3.  $\square$

**Remark 5.** We expect that for most values of  $\beta$  the tongues in the  $(\tau, \sigma)$ -parameter plane are non-degenerate, that is they intersect transversely at the vertices. We even expect this for  $Z(t) = \frac{1}{2}(1 + \sin(2\pi t))$ , since in the standard form of  $F, R_\nu$  will have a Fourier series rather than a Fourier polynomial. Also see [43].  $\square$

Let us now look at the position of the main tongue. We assume that the Zeitgeber has the following Fourier series:

$$Z(t) = c_0 + c_1 \sin(2\pi t) + \sum_{k>1} c_k \sin(2\pi(kt + \gamma_k)), \tag{6}$$

with coefficients  $c_k \in \mathbb{R}$  and  $\gamma_k \in [0, 1]$ . Note that by a time shift we can always achieve that  $\gamma_1 = 0$ . Then we have the next result.

**Proposition 5 (Boundaries of the Main Tongue).** *Let the Zeitgeber be as in Eq. (6); then the boundaries of the main tongue of the map  $F_{\mu(\nu)}$  are given by*

$$\begin{aligned} \tau_\pm &= 1 - \sigma[c_0(\cos \beta - \sin \beta) \mp c_1\sqrt{1 - \cos(2\alpha\pi) \sin(2\beta)}] \\ &\quad + \mathcal{O}(\sigma^2). \end{aligned} \tag{7}$$

For our standard example of a Zeitgeber  $Z(t) = \frac{1}{2}(1 + \sin(2\pi t))$ , the boundaries of the main tongue are given by Eq. (7) with  $c_0 = c_1 = \frac{1}{2}$  and without the  $\mathcal{O}(\sigma^2)$  term because all other coefficients are equal to zero.

### 4.3. Fixed points of the diffeomorphism $f_\mu$

Existence of stable fixed points of the circle diffeomorphism  $f_\mu$  is one of the main questions. Recall that such points correspond to entrainment in the biological model. Therefore we take a closer look at such points. From the previous sections we know that fixed points exist for parameter values in the main tongue. They are easily characterized as follows:  $t = t^*$  is a fixed point of  $f_\mu$  if  $f_\mu(t^*) = t^*$ . However, as noted before, for practical computations it is more convenient to use a lift  $F_\mu$  of  $f_\mu$ . Using the notation from Proposition 2 a point  $t = t^*$  is a fixed point of  $f_\mu$  if

$$F_\mu(t^*) = t^* + 1,$$

which is equivalent to

$$U_\varepsilon(t^* + \alpha) - \alpha + \tau = U_\eta(t^* + 1). \tag{8}$$

Even if  $\varepsilon$  and  $\eta$  are small enough that  $U_\varepsilon$  and  $U_\eta$  are invertible, this equation has several solution branches. Therefore we cannot solve (8) explicitly for  $t^*$ . Since we are mostly interested in the dependence of  $t^*$  on  $\tau$  we shall content ourselves with

$$\tau = U_\eta(t^*) - U_\varepsilon(t^* + \alpha) + \alpha + 1. \tag{9}$$

Thus for fixed values of  $\varepsilon, \eta$  and  $\alpha$  we obtain  $\tau$  as a function of  $t^*$ .

Now that we have characterized the fixed points of  $f_\mu$ , let us determine their stability. The fixed point  $t = t^*$  is stable if  $|F'_\mu(t^*)| < 1$ . After a short computation we find that

$$F'_\mu(t^*) = \frac{U'_\varepsilon(t^* + \alpha)}{U'_\eta(t^*)}. \tag{10}$$

From Eqs. (9) and (10) we almost immediately obtain an alternative characterization of stability of the fixed point  $t^*$ . Two examples of application of the following lemma are given in Fig. 5.

**Lemma 6 (Stability).** *On solution branches of Eq. (8), the fixed point  $t^*$  is stable or unstable when  $t^*$  as a function of  $\tau$  is increasing or decreasing.*

Let us again consider our standard Zeitgeber  $Z(t) = \frac{1}{2}(1 + \sin(2\pi t))$ . For fixed  $\varepsilon, \eta$  and  $\alpha$  there are two values  $t_1^*$  and  $t_2^*$  for which  $|F'_\mu(t_1^*)| = 1$  and  $|F'_\mu(t_2^*)| < 1$  if  $t^* \in [t_1^*, t_2^*]$ . We recover the boundaries of the main tongue by setting  $\tau_i = U_\eta(t_i^*) - U_\varepsilon(t_i^* + \alpha) + \alpha + 1$ ; then a stable and an unstable fixed point of the map  $f_\mu$  exist for  $\tau$  on the interval  $[\tau_1, \tau_2]$ . Motivated by this example one could conjecture that for every 1-periodic Zeitgeber with only two extrema in one period there are precisely two fixed points for parameter values in the main tongue. This turns out to be true when an extra condition is imposed.

**Proposition 7 (Number of Fixed Points).** *Let  $Z$  be a 1-periodic Zeitgeber with one maximum and one minimum on the interval  $(0, 1)$ . Then the circle map  $f_\mu$  has precisely two fixed points for parameter values in the main tongue if  $(Z'')^2 - Z' \cdot Z'''$  does not change sign.*

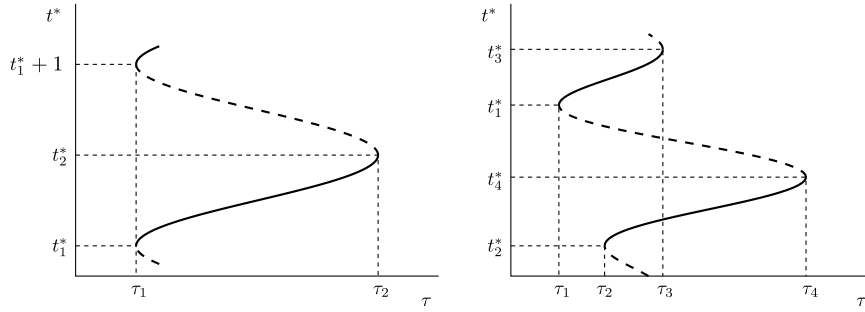


**Fig. 5.** Fixed points  $t^*$  of the map  $f_\mu$  as a function of  $\tau$ . The solid curve represents a stable fixed point, the dashed curve an unstable one. At parameter values  $\tau = \tau_i$  there are saddle-node bifurcations; also see Fig. 3. Parameters  $\varepsilon$ ,  $\eta$  and  $\alpha$  are fixed. Left: the Zeitgeber is  $Z(t) = \frac{1}{2}(1 + \sin(2\pi t))$ . Right: the Zeitgeber is  $Z(t) = \frac{3}{10}(2 + \sin(2\pi t) + \cos(4\pi t))$ .

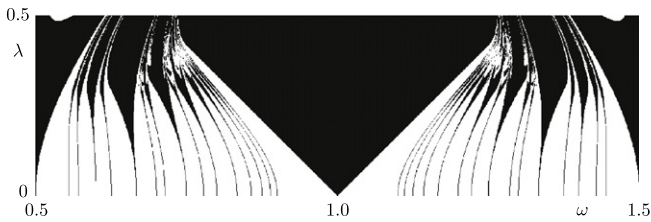


**Fig. 6.** Tongues for the Arnol'd map  $A_{\omega, \lambda}$  in the  $(\omega, \lambda)$ -plane. The algorithm for computing the pictures is based on the rotation number. The latter is defined for sufficiently small values of  $\lambda$  only. Therefore the tongue boundaries in the picture are not well defined for large values of  $\lambda$ . The effect of this phenomenon is even more visible in the following picture.

For our standard example of a Zeitgeber  $Z(t) = \frac{1}{2}(1 + \sin(2\pi t))$ , the quantity  $(Z'')^2 - Z' \cdot Z'''$  is equal to 1. The Zeitgeber  $Z(t) = \frac{2}{5}(\frac{4}{3} + \sin(2\pi t) + \frac{1}{3}\sin(4\pi t))$  also has two extrema, but the quantity  $(Z'')^2 - Z' \cdot Z'''$  changes sign on  $[0, 1]$ . See the Appendix for further implications. With a general periodic Zeitgeber there may be more than one stable fixed point for parameter values in the main tongue. This occurs in general when the Fourier series of the Zeitgeber contains more than just one term like in our standard example. Let us look at a Zeitgeber with the following Fourier polynomial:  $Z(t) = \frac{3}{10}(2 + \sin(2\pi t) + \cos(4\pi t))$ ; then there are four solutions of  $|F'_\mu(t_i^*)| = 1$ . Let us sort them such that  $\tau_i = U_\eta(t_i^*) - U_\varepsilon(t_i^* + \alpha) + \alpha + 1$  increases with  $i$ . Then for fixed values of  $\varepsilon$ ,  $\eta$  and  $\alpha$  there are at most four fixed points of  $f_\mu$  for each  $\tau \in [\tau_1, \tau_4]$ . We represent the results graphically in Fig. 5.

4.4. Examples of tongues and hairs for different Zeitgebers

Here we collect some examples of tongues-and-hairs figures showing differences from and similarities with the prototype figure of tongues in the Arnol'd circle map. Therefore we start with the latter; see Fig. 6. In this family the tongues are fixed, but in our family  $f_\mu$ , the tongues in the  $(\tau, \sigma)$ -plane still depend on the values of  $\beta$  and  $\alpha$ . Moreover they also depend on the Zeitgeber. In order to keep the number of pictures limited we only show tongues for two different Zeitgebers; see Figs. 7 and 8. As is to be expected from the existence of a standard form (see Section 4.2), the pictures are qualitatively the same—that is, near the  $\tau$ -axis or  $\omega$ -axis in the Arnol'd map. The width and the growth of the width of the tongues depend on parameters in the map. This is shown in Fig. 9, in the next section, where its biological relevance is discussed.

5. Discussion

The main results of analyzing our model for a pacer cell with a periodic Zeitgeber are:

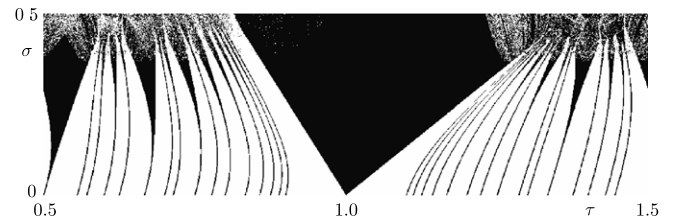


**Fig. 7.** Tongues for the circle map  $f_\mu$  in the  $(\tau, \sigma)$ -plane, with standard Zeitgeber  $Z(t) = \frac{1}{2}(1 + \sin(2\pi t))$ . The values of the parameters  $\mu = (\varepsilon, \eta, \alpha, \tau)$  are  $\varepsilon = \sigma \cos \beta$ ,  $\eta = \sigma \sin \beta$  with  $\beta = \frac{\pi}{3}$  and  $\alpha = 0.3$ .

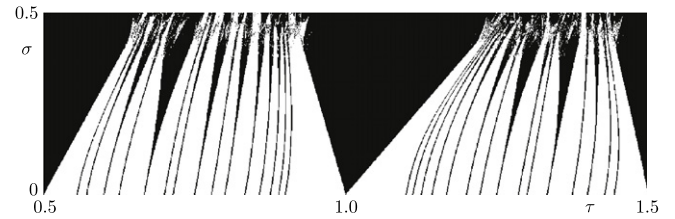


**Fig. 8.** Tongues for the circle map  $f_\mu$  in the  $(\tau, \sigma)$ -plane, with Zeitgeber  $Z(t) = \frac{3}{10}(2 + \sin(2\pi t) + \cos(4\pi t))$ . The parameter values are as in Fig. 7.

1. there is a finite range of entrainment, namely the 1:1 tongue,
2. there are finite ranges of synchronization in the more general  $p : q$  tongues,
3. the boundaries of the range of entrainment depend on the phase delay and advance parameters in the model,
4. outside the tongues the pacer cell shows quasi-periodic behavior, known as relative coordination in circadian biology,
5. the phase of entrainment, or onset of activity interval, depends on the intrinsic period of the pacer cell.

In the following sections we will discuss these matters in more detail. Let us remark that ranges of synchronization and entrainment apply to the intrinsic period, while the period of the Zeitgeber is kept fixed. From a biological point of view it seems more natural to keep the intrinsic period fixed and vary the period of the Zeitgeber. However, it is not hard to see that these viewpoints are in fact equivalent.

5.1. The model

As explained in Section 2 our long-term goal is to study a collection of interacting pacer cells with a Zeitgeber acting as an external stimulus. However, there are serious difficulties in the analysis of the mathematical model that is induced by this biological model; again see Section 2. Therefore we consider a simpler system of a single pacer cell that experiences stimuli from other pacer cells as well as external sources. We regard the sum of

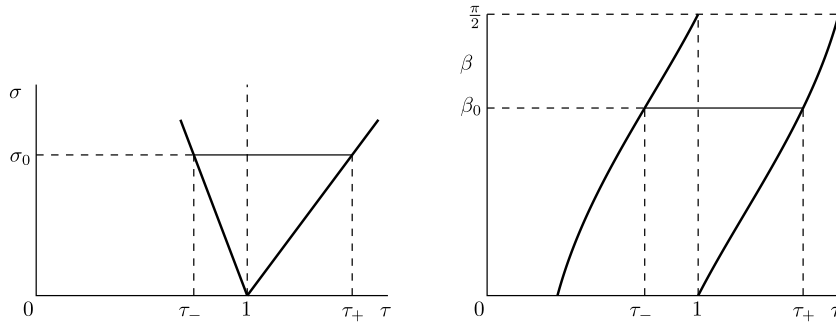


**Fig. 9.** Left: the main tongue of the circle map  $f_\nu$ , where  $\nu = (\sigma, \beta, \alpha, \tau)$  with  $\alpha = 0.3$  and  $\beta = \beta_0$  fixed. For  $\sigma = \sigma_0$  the range of entrainment is the width of the tongue at  $\sigma = \sigma_0$ , namely the interval  $(\tau_-, \tau_+)$ . Right: the range of entrainment  $(\tau_-, \tau_+)$  for fixed  $\sigma = \sigma_0$  and  $\beta$  varying in  $(0, \frac{\pi}{2})$ . The parameter  $\beta$  determines the ratio of  $\varepsilon$  and  $\eta$  since  $\varepsilon = \sigma \cos \beta$  and  $\eta = \sigma \sin \beta$ .

all such stimuli as the Zeitgeber for the single pacer cell. The latter, in this simplification, does not stimulate the other pacer cells. In physics this is known as the mean field approach. Our analysis first focuses on periodic Zeitgebers. Under these conditions we naturally obtain a dynamical system consisting of a circle map for this biological model. The heart of the mathematical model is the circle map  $f_\mu$  that yields, once  $t_0$  is given, a sequence of relative times  $t_n$  corresponding to the beginning of an activity interval of the pacer cell. The sequence  $t_0, t_1 = f_\mu(t_0), t_2 = f_\mu(t_1), \dots$  is called the itinerary of  $t_0$ . In this setting, time is relative to the period  $T$  of the periodic Zeitgeber that acts as a stimulus to the pacer cell. It is convenient to use  $T$  as a unit of time; that is, we scale time such that  $T = 1$ . The circle map  $f_\mu$  depends on parameters  $\mu = (\varepsilon, \eta, \alpha, \tau)$ , where  $\tau$  is the intrinsic period of the pacer cell, measured in the time unit  $T = 1$ . Furthermore  $\varepsilon$  and  $\eta$  determine the phase delay and phase advance, and  $\alpha$  determines the length of the intrinsic activity interval; see Section 2 for an explanation of these terms.

5.2. Dynamics

In the description of the dynamical behavior of the map  $f_\mu$  there is a difference between  $f_\mu$  being invertible (diffeomorphic) and not being invertible. We mainly restrict to the invertible case. Furthermore we restrict to *typical dynamics*; see [39] for a precise definition. In the present case this comprises fixed points, periodic points and quasi-periodic points. Note that the itinerary of the latter consists of an infinite sequence.

The simplest kind of dynamics is a fixed point of  $f_\mu$ , which means that the activity interval of the pacer cell always starts at the same relative time. The existence of such points implies the possibility of entrainment. The next simplest kind of dynamics is a periodic point of  $f_\mu$ . This means that there is a  $t_0$  such that in the sequence  $t_0, t_1 = f_\mu(t_0), \dots, t_q = f_\mu(t_{q-1})$  the last point  $t_q$  is again equal to  $t_0$  for some fixed  $q$ . In general these  $q$  onsets of activity occur in  $p$  periods of the Zeitgeber. We call this synchronization of the pacer cell, a generalization of entrainment. The periodic point  $t_0$  is called  $p : q$  periodic. The last kind of typical dynamics for the map  $f_\mu$  is quasi-periodicity. The point  $t_0$  is quasi-periodic if the itinerary of  $t_0$  densely fills the circle or interval  $[0, 1]$  depending on how we represent the map.

The kind of dynamics that the map  $f_\mu$  exhibits depends on the values of the parameters. All this is nicely organized in parameter space in wedge shaped regions called tongues, one for each pair  $(p, q)$ ; see Fig. 3. However, here we need the restriction that  $f_\mu$  is invertible. For parameter values in the  $(p, q)$  tongue, the typical dynamics of  $f_\mu$  is  $p : q$ -periodicity. A special role is played by the tongue for  $(p, q) = (1, 1)$ , called the main tongue. Fixed points are the typical dynamics of  $f_\mu$  for parameter values in the main tongue. At the boundaries of the tongues, the map  $f_\mu$  has a saddle-node bifurcation; see Section 4.1. For parameter values outside the

tongues the dynamics of the map is quasi-periodic; this occurs on hairs in the  $(\tau, \sigma)$ -parameter plane. If  $f_\mu$  is not invertible, tongues still exist but generally overlap, so coexistence of periodic points with different periods becomes possible.

5.3. Entrainment

For parameter values in the main tongue, the tongue with  $(p, q) = (1, 1)$ , the map  $f_\mu$  has fixed points. There are at least two such points; of these, one is stable and the other is unstable. The stable one corresponds to entrainment of the pacer cell. Let us discuss the shape of the main tongue in some more detail to find the parameter values for which entrainment occurs.

The parameter space is four dimensional and in it tongue boundaries are hyper-surfaces. The situation becomes simpler if we do not use coordinates  $(\varepsilon, \eta, \alpha, \tau)$  but  $(\sigma, \beta, \alpha, \tau)$  with  $\varepsilon = \sigma \cos \beta$  and  $\eta = \sigma \sin \beta$ . Then  $\sigma$  satisfies  $\sigma^2 = \varepsilon^2 + \eta^2$  and measures how strongly the Zeitgeber stimulates the pacer cell, while  $\beta$  determines the ratio of  $\varepsilon$  and  $\eta$ . In these coordinates in parameter space the boundaries of the main tongue are given by Eq. (7). As we can see from the standard form in Theorem 4, the main parameters are  $\tau$  and  $\sigma$ . In the  $(\tau, \sigma)$ -plane we find the tongues (see Fig. 9) whose detailed shape depends on  $\alpha$  and  $\beta$ . The range of entrainment is given by the interval  $(\tau_-, \tau_+)$ , with  $\tau_\pm$  given in equation Eq. (7), when other parameters are kept fixed. There are many biological experiments/observations supporting the existence of bounded ranges of entrainment; see [3]. In practice one cannot vary the intrinsic period  $\tau$  of the pacer cell. But varying the period of the Zeitgeber  $T$  at a fixed value of  $\tau$  is equivalent to varying  $\tau$  and fixing  $T$  in the model; see [29,38,35]. However, biological evidence exists that the intrinsic period varies among individual pacer cells while they can still entrain to a Zeitgeber with a 24 h period; see [44,9,45,33,11].

In Section 4.3 on fixed points of the map  $f_\mu$  we noted that the position of stable fixed points is an increasing function of the intrinsic period  $\tau$ . This has been observed by various authors (for example see [28,46]) and for particular organisms by Aschoff [2], Aschoff and Pohl [29], Daan and Pittendrigh [23], and Roenneberg and Merrow [38]. In Fig. 10 we show data from [38] essentially giving the relative onset times of the activity interval as a function of the intrinsic period for several mutants of the fungus *Neurospora crassa*.

Both the position and the length of the interval  $(\tau_-, \tau_+)$  depend on  $\alpha$  and  $\beta$ . As we see from Fig. 9 the range of entrainment is in general not centered at  $\tau = 1$ . Here  $\beta$  is the most important parameter. If  $\beta < \frac{\pi}{4}$  or equivalently  $\varepsilon > \eta$ , then the phase delay is larger than the phase advance and the range of entrainment is shifted towards intrinsic periods  $\tau$  smaller than the period  $T$  of the Zeitgeber. If  $\beta > \frac{\pi}{4}$ , the range of entrainment is shifted in the direction of intrinsic periods  $\tau$  larger than the period  $T$  of the



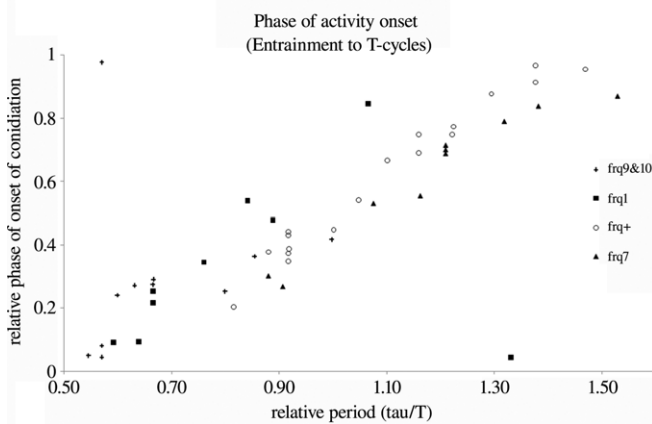


**Fig. 10.** Relative times of onset of activity interval for four mutants of *Neurospora crassa*. The genetic types are indicated by markers; see [38] for an explanation of *frq1*, *frq+*, *frq7* and *frq9* and *10*.

Zeitgeber. The model has two extreme cases. One is for  $\beta = 0$  or equivalently  $\eta = 0$  (only phase delay), where only pacer cells with intrinsic period  $\tau$  less than the period  $T$  of the Zeitgeber can be entrained. The other one is for  $\beta = \frac{\pi}{2}$  or equivalently  $\varepsilon = 0$  (only phase advance), where  $\tau$  must be larger than  $T$  for entrainment to occur. A phenomenon related to this skewness has been observed for several nocturnal rodents [23] where a decreasing center of the range of entrainment corresponds to increasing phase delay and decreasing phase advance.

As mentioned before, in the main tongue, the map  $f_\mu$  has at least a pair of fixed points, one stable and one unstable. However more pairs may exist, leading to curves of saddle-node bifurcations inside the main tongue; see Fig. 5. Thus upon varying  $\tau$ , a fixed point may lose its stability and the system then jumps to another stable fixed point. As long as parameter values remain in the main tongue this is the only possibility. Another possibility is to keep the parameters  $\mu$  fixed but vary a parameter in the Zeitgeber. For a biological example possibly related to such a mechanism, see [47].

#### 5.4. Synchronization

Apart from entrainment, the model also shows the possibility of the more general phenomenon called synchronization. This occurs for parameter values in the  $p : q$  tongues in the  $(\tau, \sigma)$ -plane. Then the circle map  $f_\mu$  has a  $q$ -periodic orbit consisting of points  $t_0, t_1, \dots, t_{q-1}$  indicating the beginnings of  $q$  activity intervals of the pacer cell in  $p$  periods of the Zeitgeber. In the  $p : q$  tongues we have the same phenomena as in the main tongue; the only difference is that they apply to periodic points instead of fixed points.

There is an example of a 2:1 periodic point: the fungus *Neurospora sp* has one activity interval in two periods of the Zeitgeber; see [31]. Here the Zeitgeber is a temperature stimulus.

#### 5.5. No synchronization

For parameter values outside the tongues the circle map has quasi-periodic orbits. This corresponds to quasi-periodic occurrence of activity intervals of the pacer cell. In practice such behavior may be hard to distinguish from periodic behavior with a long period. In circadian biology, such loss of entrainment often leads to a phenomenon called relative coordination. An example of such behavior is provided by the daily activity of chaffinch which shows an alternation of seemingly entrained and free running behaviors [2].

#### 5.6. Future directions

There are several ways to generalize or extend the current model for a single pacer cell with a periodic Zeitgeber. We first concentrate on the biological model of Section 2 in view of our future goal of describing a collection of interacting pacer cells, stimulated by a Zeitgeber.

*Single pacer cell, circle map.* In the present analysis we restricted to the case where the map  $f_\mu$  is a circle diffeomorphism (invertible map). Then the  $(\tau, \sigma)$ -plane is divided into tongues with well-defined periodic dynamics and hairs with quasi-periodic dynamics. This only occurs when the stimulus of the Zeitgeber on the pacer cell is relatively weak. Allowing a stronger stimulus, the map  $f_\mu$  becomes an endomorphism (non-invertible map) with far richer bifurcation scenarios; see for example [43]. However, it is not clear whether the subtleties of the endomorphism case are in accordance with the coarseness of the underlying biological model. Therefore we restrict to the simplest properties of each model.

*Single pacer cell, torus map.* Thus it seems more fruitful to generalize in another direction and consider a quasi-periodic Zeitgeber. This will lead to a torus map instead of a circle map. Such a generalization is also more relevant for our aim of studying a collection of pacer cells, by first considering a single cell with an asymmetric interaction with its environment. The latter stimulates the pacer cell, but not vice versa.

*Collection of pacer cells, no interaction.* In a model for a collection of pacer cells we can already use the results for a single cell. As a first model let us assume that the cells are stimulated by an external periodic Zeitgeber but do not interact. Although biologically not particularly relevant, it is a step in gradually sophisticating the model. Furthermore suppose that there are  $n$  cells, characterized by parameter values  $(\varepsilon_i, \eta_i, \alpha_i, \tau_i)$  in the main tongue for  $i = 1, \dots, n$ . That is, we apply the current single pacer cell model for each cell. Then the collection will be entrained to the Zeitgeber, although each cell has its own onset time and length of activity interval. The collective behavior, though, will be periodic.

*Collection of pacer cells, with interaction.* We conjecture that, starting with the previous model, for a sufficiently weak interaction there will still be entrainment. Nevertheless it will be interesting to consider a model for interacting pacer cells without a Zeitgeber as well. Here we may take the pacer cells nearly identical in the sense of the previous paragraph. However there is biological evidence that there are different kinds of pacer cells [9–11]. In further extensions one could again include a periodic Zeitgeber. Since in a model for a collection of pacer cells the Zeitgeber acts solely as an external stimulus, it seems most natural to restrict to periodic Zeitgebers. However we may wish to include both daily and seasonal variations. This would imply that the period of the Zeitgeber is a year. Another possibility is to stick to Zeitgebers with a 24 h period and use methods for slowly varying parameters to include seasonal changes.

*Non-periodic pacer cells.* As mentioned before (see Section 1), there is experimental evidence that not all pacer cells, or more precisely cells from the suprachiasmatic nucleus, show periodic behavior. Despite that, they may still contribute to entrainment to a periodic Zeitgeber. This is again a different aspect not present in the current model. One direction is to consider pacer cells that can be modeled as quasi-periodic or even more general oscillators. Another direction is to model each as a system with an a priori stationary state that may undergo a Hopf bifurcation when the strength of the interaction with the Zeitgeber increases. In the former, entrainment can possibly only be realized approximately, but in the latter, entrainment, in a strict sense, is still conceivable.

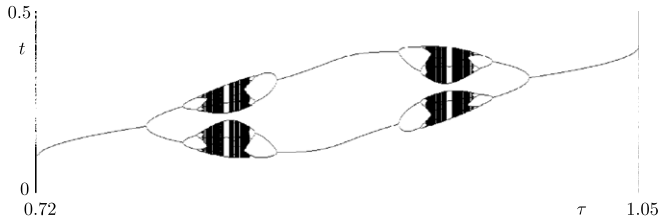


**Fig. 11.** Period doublings and halvings for the map  $f_\mu$  with Zeitgeber  $Z(t) = 3 + \sin(2\pi t) + 2 \cos(4\pi t)$ . Shown are the positions of periodic points as a function of the intrinsic period  $\tau$ . The parameter values are  $\alpha = 0.5$ ,  $\varepsilon = 0.4$  and  $\eta = 0.17$ .

## 6. Conclusion

The current model has been used to explain many properties of the mammalian circadian behavior [14]. In addition, we provided the mathematical basis using the current model of at least five phenomena that are characteristic of circadian behavior in general: (1) finite range of entrainment; (2) existence of multiple activity bouts per cycle ( $p : q$  tongues); (3) relative coordination or cycles with extremely long periods (quasi-periodic orbits); (4) relationship of the phase of entrainment to the period of the Zeitgeber; (5) asymmetry in the observed period and the phase delay and phase advance components of phase response curves. Aside from these, we also now have a set of four directly observable parameters to look at more closely in biological systems. Most experiments in the past have only searched for genes and proteins responsible for the intrinsic period  $\tau$ . However, circadian clocks are also characterized by their phase response curves which in the simple pacemaker model are defined with only three more basic parameters  $\alpha$ ,  $\varepsilon$ ,  $\eta$ . We think that an important predictive value of the current work is our discovery of the mathematical relationships between these four parameters and their contribution to various aspects of entrainment. Now, one direction that biologists should pursue is to do extensive experimentation to search in the complex biochemical system for molecular components which could be responsible for the phase delay and phase advance parameters  $\varepsilon$  and  $\eta$ , respectively, as well as the intrinsic activity length  $\alpha$ . Finally, one may say that the model is too simple to capture the entire phase response characteristics of whole organisms, or even of a single pacemaker cell. The PRC used must be rather realistic for an individual pacemaker cell, at least if our assumption that the behavior can be characterized by two states (electrical activity versus rest) is correct. The result of the interactions between the various pacemaker cells and their response to light will eventually lead to the known PRCs of the ensemble, in which phase delays occur at the end of the photoperiod and advances at the beginning. However, we must emphasize that even this very simple model with only four parameters already captures those characteristics mentioned above, that is, we did not use a more realistic phase response curve [23] to simulate those characteristics. Properties that we can see in the model such as hysteresis (see Fig. 5) and period-halving and period-doubling cascades (see Fig. 11) remain to be seen in experiments at the behavioral and lower levels. The underlying biochemical network that produces these four parameters may just be details that are not really necessary in understanding entrainment of circadian rhythms itself, but have important roles in other aspects of the biological system such as energy expenditure and adaptation to changes in environment [1].

## Acknowledgments

We would like to thank the anonymous referees of Physica D for their constructive criticism and valuable suggestions. These have been very useful in improving the paper.

## Appendix A. Bifurcations

The tongues in the  $(\sigma, \tau)$ -parameter plane are determined by saddle-node bifurcations. But there may also be other bifurcations even when the map  $f_\mu$  is a diffeomorphism, in other words invertible. The reason is that we have many parameters. Considering  $\alpha$  as a relatively inaccessible parameter and keeping it fixed we may still vary  $\sigma$ ,  $\tau$  and  $\beta$ . Then we have three-dimensional tongues in  $(\sigma, \tau, \beta)$ -parameter space. It is an almost straightforward consequence of Proposition 7 that there are curves of pitchfork bifurcations in this three-dimensional parameter space, emanating from rational points on the  $\tau$ -axis.

**Corollary 8 (Pitchfork Bifurcation).** *Let  $Z$  be a 1-periodic Zeitgeber. If  $(Z'')^2 - Z' \cdot Z'''$  has a simple zero, then parameter values exist for which  $f_\mu$  has a pitchfork bifurcation.*

**Proof.** From the proof of Proposition 7 we see that the number of solution branches of Eq. (8) does change if  $Z''(t)^2 - Z'(t) \cdot Z'''(t)$  has a simple zero.  $\square$

However,  $\beta$  may be considered as an inaccessible parameter as well. But the Zeitgeber may also depend on a parameter. We may in particular view seasonal change, which is slow compared to the 24 h period, as parameter dependence. The quantity  $(Z'')^2 - Z' \cdot Z'''$  may change sign depending on this parameter, so we find again pitchfork bifurcations.

If the map  $f_\mu$  is not a diffeomorphism (not invertible) then there are numerous other bifurcations; see [43]. This happens for relatively large values of  $\sigma$ . On varying  $\tau$  for fixed values of the other parameters in the main tongue, one generally finds a number of period doublings followed by the same number of period halvings (or in opposite order). The reason is that there are curves of period doublings in the  $(\tau, \sigma)$ -parameter plane with local minima, considered as functions of  $\tau$ , that are transversely crossed. For more details we refer the reader again to [43]. An example of this phenomenon is shown in Fig. 11.

## Appendix B. Proofs

**Proof of Proposition 2.** The main point we have to show is that Eq. (2) can be solved uniquely with respect to  $t$ . Using the expression for  $\theta$  in (1) we obtain after some rearranging

$$t_{n+1} + \eta Z(t_{n+1}) = t_n + \alpha + \varepsilon Z(t_n + \alpha) - \alpha + \tau. \quad (11)$$

Since  $Z$  is 1-periodic,  $U_\varepsilon$  has the property  $U_\varepsilon(t + 1) = U_\varepsilon(t) + 1$ , for all  $t$ . Then the equation for  $t_{n+1}$  reads

$$U_\eta(t_{n+1}) = U_\varepsilon(t_n + \alpha) - \alpha + \tau.$$

Introducing the operator  $\mathcal{T}_\alpha$  which takes a function  $f$  into  $\mathcal{T}_\alpha f = T_{-\alpha} \circ f \circ T_\alpha$  where  $T_\alpha$  is just a translation over  $\alpha$ , that is  $T_\alpha(t) = t + \alpha$ , we can write the equation for  $t_{n+1}$  as

$$U_\eta(t_{n+1}) = \mathcal{T}_\alpha U_\varepsilon(t_n) + \tau. \quad (12)$$

Solvability of (12) depends on the value of  $\eta$ . If  $\eta$  is small enough,  $U_\eta$  is invertible and we write

$$t_{n+1} = F_\mu(t_n) = U_\eta^{-1}(\mathcal{T}_\alpha U_\varepsilon(t_n) + \tau).$$

Then  $F_\mu$  is a differentiable map with the property  $F_\mu(t + 1) = F_\mu(t) + 1$ , which means that  $F_\mu$  is the lift of a circle map of degree 1. Note that  $F_\mu$  depends on the parameters  $\mu = (\varepsilon, \eta, \alpha, \tau)$ .  $\square$

**Proof of Theorem 4.** A consequence of  $F_\mu(t + 1) = F_\mu(t) + 1$  is that  $F_\mu(t) - t$  is 1-periodic; thus there is a 1-periodic  $C^\infty$  function  $P_\nu$  such that  $F_\mu(t) = t + P_\nu(t)$ .  $P_\nu$  has a Fourier series so we may split off the constant term and we write  $P_\nu(t) = \omega(\nu) + Q_\nu(t)$  with  $\omega(\nu) = \int_0^1 P_\nu(t) dt$ ; then  $\omega$  is a  $C^\infty$  function of  $\nu$ . Furthermore  $Q_\nu(t) = P_\nu(t) - \omega(\nu)$  so  $Q_\nu$  is a 1-periodic  $C^\infty$  function with  $\int_0^1 Q_\nu(t) dt = 0$ . So far,  $F_\mu(t) = t + \omega(\nu) + Q_\nu(t)$ . For  $\sigma = 0$  we have  $F_\mu(t) = t + \tau$ , so  $\omega(0, \beta, \alpha, \tau) = \tau$  and  $Q_{(0, \beta, \alpha, \tau)}(t) = 0$ . Using the division property of  $C^\infty$  functions, a 1-periodic,  $C^\infty$  function  $R_\nu$  exists such that  $Q_\nu(t) = \sigma R_\nu(t)$ . Finally  $F_{(\sigma \cos \beta, \sigma \sin \beta, \alpha, \tau)}(t) = t + \omega(\nu) + \sigma R_\nu(t)$ .  $\square$

**Proof of Proposition 5.** Recall that  $\mu = (\varepsilon, \eta, \alpha, \tau)$  and  $\nu = (\sigma, \beta, \alpha, \tau)$  with  $\varepsilon = \sigma \cos \beta$  and  $\eta = \sigma \sin \beta$ . Then for small  $\sigma$  and assuming that  $1 - \tau = \mathcal{O}(\sigma)$  we get

$$\begin{aligned} F_{\mu(\nu)} &= U_{-\eta}(U_\varepsilon(t + \alpha) - \alpha + \tau) + \mathcal{O}(\sigma^2) \\ &= t + \tau + \varepsilon Z(t + \alpha) - \eta Z(t + \tau) + \mathcal{O}(\sigma^2) \\ &= t + \tau + \varepsilon Z(t + \alpha) - \eta Z(t) + \mathcal{O}(\sigma^2). \end{aligned}$$

The Zeitgeber  $Z$  has the following Fourier series:  $Z(t) = c_0 + c_1 \sin(2\pi t) + \sum_{k>1} c_k \sin(2\pi(kt + \gamma_k))$ . After a near identity transformation followed by a time shift, we obtain that  $F_{\mu(\nu)}$  is equivalent to

$$\begin{aligned} G_{\mu(\nu)}(t) &= t + \tau + (\varepsilon - \eta)c_0 + \varepsilon c_1 \sin(2\pi(t + \alpha)) \\ &\quad - \eta c_1 \sin(2\pi t) + \mathcal{O}(\sigma^2). \end{aligned}$$

It almost immediately follows that the boundaries of the main tongue of  $G$  and thus of  $F$  are as stated in the lemma.  $\square$

**Proof of Proposition 7.** The number of fixed points may change if the number of solution branches of Eq. (8),  $U_\varepsilon(t + \alpha) - \alpha + \tau = U_\eta(t + 1)$ , changes. This is equivalent to a changing number of extrema of  $\tau = U_\eta(t) - U_\varepsilon(t + \alpha) + \alpha + 1$ . Using  $U_\varepsilon(t) = t + \varepsilon Z(t)$  we get  $\tau = \eta Z(t) - \varepsilon Z(t + \alpha) + \alpha + 1$ . Thus the number of extrema of  $\tau$  changes at parameter values for which

$$\begin{cases} \eta Z'(t) - \varepsilon Z'(t + \alpha) = 0 \\ \eta Z''(t) - \varepsilon Z''(t + \alpha) = 0. \end{cases}$$

This equation has trivial solutions for  $\varepsilon$  and  $\eta$  only if  $Z'(t) \cdot Z''(t + \alpha) - Z'(t + \alpha) \cdot Z''(t) \neq 0$ . We rewrite this as

$$\frac{Z'(t)}{Z''(t)} \neq \frac{Z'(t + \alpha)}{Z''(t + \alpha)}.$$

This inequality holds if  $h(t) = \frac{Z'(t)}{Z''(t)}$  is injective. Therefore a sufficient condition is that  $h'$  does not change sign. From

$$h'(t) = \frac{Z''(t)^2 - Z'(t) \cdot Z'''(t)}{Z''(t)^2}$$

the result follows.  $\square$

**References**

[1] C.H. Johnson, Testing the adaptive value of circadian systems, *Methods in Enzymol.* 393 (2005) 818–837.  
 [2] J. Aschoff, Freerunning and entrained circadian rhythms, in: J. Aschoff (Ed.), *Biological Rhythms*, in: *Handbook of Behavioral Neurobiology*, vol. 4, Plenum Press, New York, 1981, pp. 81–93.  
 [3] S. Daan, J. Aschoff, The entrainment of circadian systems, in: Joseph S. Takahashi, Fred W. Turek, Robert Y. Moore (Eds.), *Circadian Clocks*, in: *Handbook of Behavioral Neurobiology*, vol. 12, Kluwer Academic/Plenum Publishers, New York, 2001, pp. 7–43.  
 [4] M.H. Hastings, E.D. Herzog, Clock genes, oscillators, and cellular networks in the suprachiasmatic nucleus, *J. Biol. Rhythms* 19 (2004) 400–413.  
 [5] R.Y. Moore, V.B. Eichler, Loss of a circadian corticosterone rhythm following suprachiasmatic lesions in the rat, *Brain Res.* 42 (1972) 201–206.  
 [6] R.Y. Moore, Retinohypothalamic projection in mammals: a comparative study, *Brain Res.* 49 (1973) 403–409.

[7] M.R. Ralph, R.G. Foster, F.C. Davis, M. Menaker, Transplanted suprachiasmatic nucleus determines circadian period, *Science* 247 (1990) 975–978.  
 [8] J.T. Enright, The Timing of Sleep and Wakefulness: On the Substructure and Dynamics of the Circadian Pacemakers Underlying the Wake–Sleep Cycle, Springer-Verlag, Berlin, 1980.  
 [9] S. Honma, W. Nakamura, T. Shirakawa, K. Honma, Diversity in circadian periods of single neurons in rat suprachiasmatic nucleus depends on nuclear structure and intrinsic period, *Neurosci. Lett.* 358 (2004) 173–176.  
 [10] A.B. Webb, N. Angelo, J.E. Huettnner, E.D. Herzog, Intrinsic, nondeterministic circadian rhythm generation in identified mammalian neurons, *PNAS* 106 (2009) 16493–16498.  
 [11] D.K. Welsh, D.E. Logothetis, M. Meister, S.M. Reppert, Individual neurons dissociated from rat suprachiasmatic nucleus express independently phased circadian firing rhythms, *Neuron* 14 (1995) 697–706.  
 [12] L. Yan, N.C. Foley, J.M. Bobula, L.J. Kriegsfeld, R. Silver, Two antiphase oscillations occur in each suprachiasmatic nucleus of behaviorally split hamsters, *J. Neurosci.* 25 (2009) 9017–9026.  
 [13] M.D.C. Belle, C.O. Diekmann, D.B. Forger, H.D. Piggins, Daily electrical silencing in the mammalian circadian clock, *Science* 326 (2009) 281–284.  
 [14] D.G.M. Beersma, B.A.D. van Bunnik, R.A. Hut, S. Daan, Emergence of circadian and photoperiodic system level properties from interactions among pacemaker cells, *J. Biol. Rhythms* 23 (2008) 362–373.  
 [15] R.E. Mrolo, S.H. Strogatz, Synchronization of pulse-coupled biological oscillators, *SIAM J. Appl. Math.* 50 (1990) 1645–1662.  
 [16] C.P. Fall, *Computational Cell Biology*, in: *Interdisciplinary Applied Mathematics*, vol. 20, Springer-Verlag, New York, 2002.  
 [17] D. Gonze, S. Bernard, C. Waltermann, A. Kramer, H. Herzel, Spontaneous synchronization of coupled circadian oscillators, *Biophys. J.* 89 (2005) 120–129.  
 [18] B.C. Goodwin, Oscillatory behavior in enzymatic control processes, *Adv. Enzyme. Regul.* 3 (1965) 425–438.  
 [19] H.P. Mirsky, A.C. Liu, D.K. Welsh, S.A. Kay, F.J. Doyle, III, A model of the cell-autonomous mammalian circadian clock, *PNAS* 106 (27) (2009) 11107–11112.  
 [20] J. Wang, T. Zhou, cAMP-regulated dynamics of the mammalian circadian clock, *BioSystems* 101 (2010) 136–143.  
 [21] V.I. Arnold, *Geometrical Methods in the Theory of Ordinary Differential Equations*, Springer-Verlag, New York, 1983.  
 [22] A. Granada, R.M. Hennig, B. Ronacher, A. Kramer, H. Herzel, Phase response curves: elucidating the dynamics of coupled oscillators, *Methods in Enzymology* 454 (2009) (Chapter 1).  
 [23] S. Daan, C.S. Pittendrigh, A functional analysis of circadian pacemakers in nocturnal rodents, II. Variability of phase response curves, *J. Comparative Phys. A* 106 (1976) 253–266.  
 [24] A.T. Winfree, Biological rhythms and the behavior of populations of coupled oscillators, *J. Theoret. Biol.* 16 (1967) 15–42.  
 [25] L. Glass, Synchronization and rhythmic processes in physiology, *Nature* 410 (2001) 277–284.  
 [26] L. Glass, J. Sun, Periodic forcing of a limit cycle oscillator: fixed points, Arnold tongues and the global organization of bifurcations, *Phys. Rev. E* 50 (6) (1994) 5077–5084.  
 [27] M.E. Jewett, R.E. Kronauer, Refinement of a limit cycle oscillator model of the effects of light on the human circadian pacemaker, *J. Theor. Biol.* 192 (1998) 344–354.  
 [28] J. Aschoff, Response curves in circadian periodicity, in: Jürgen Aschoff (Ed.), *Circadian Clocks: Proceedings of the Feldafing Summer School*, North-Holland Publishing Company, Amsterdam, 1965, pp. 95–111.  
 [29] J. Aschoff, H. Pohl, Phase relations between a circadian rhythm and its Zeitgeber within the range of entrainment, *Naturwissenschaften* 23 (1978) 80–84.  
 [30] R.A. Hut, B.E.H. van Oort, S. Daan, Natural entrainment without dawn and dusk: the case of the European ground squirrel (*Spermophilus citellus*), *J. Biol. Rhythms* 14 (1999) 290–299.  
 [31] M. Mroow, C. Boesl, J. Ricken, M. Messerschmitt, M. Goedel, T. Roenneberg, Entrainment of the Neurospora circadian clock, *Chronobiol. Internat.* 23 (2006) 71–80.  
 [32] S. Daan, C.S. Pittendrigh, A functional analysis of circadian pacemakers in nocturnal rodents, IV. Entrainment: Pacemaker as Clock, *J. Comparative Phys. A* 106 (1976) 291–331.  
 [33] T. Shirakawa, S. Honma, Y. Katsuno, H. Oguchi, K. Honma, Synchronization of circadian firing rhythms in cultured rat suprachiasmatic neurons, *Eur. J. Neurosci.* 12 (2000) 2833–2838.  
 [34] S.H. Strogatz, SYNC: the emerging science of spontaneous order, *Hyperion* (2003).  
 [35] S. Usui, Y. Takahashi, T. Okazaki, Range of entrainment of rat circadian rhythms to sinusoidal light-intensity cycles, *Am. J. Physiol. Regul. Integrative Comparative Phys.* 278 (2000) R1148–1156.  
 [36] R. Wever, The duration of re-entrainment of circadian rhythms after phase shifts of the zeitgeber, *J. Theoret. Biol.* 13 (1966) 187–201.  
 [37] R. Wever, Internal phase-angle differences in human circadian rhythms: causes for changes and problems of determinations, *Int. J. Chronobiol.* 1 (1973) 371–390.  
 [38] T. Roenneberg, M. Mroow, The role of feedbacks in circadian systems, in: K. Honma, S. Honma (Eds.), *Zeitgebers, Entrainment, and Masking of the Circadian System*, Hokkaido Univ. Press, Sapporo, 2001, pp. 113–129.  
 [39] H.W. Broer, F. Takens, *Dynamical Systems and Chaos*, in: *Appl. Math. Sci.*, vol. 172, Springer, 2010.  
 [40] R.L. Devaney, *An Introduction to Chaotic Dynamical Systems*, Benjamin-Cummings, 1986.  
 [41] A. Katok, B. Hasselblatt, *Introduction to the Modern Theory of Dynamical Systems*, Cambridge University Press, 1997.

- [42] Y.A. Kuznetsov, Elements of Applied Bifurcation Theory, 3rd ed., in: Applied Mathematical Sciences, vol. 112, Springer, Berlin, 2004.
- [43] H.W. Broer, C. Simó, J.C. Tatjer, Towards global models near homoclinic tangencies of dissipative diffeomorphisms, *Nonlinearity* 11 (1998) 667–770.
- [44] K. Honma, S. Honma, T. Hiroshige, Response curve, free-running period, and activity time in circadian locomotor rhythm of rats, *Japan. J. Phys.* 35 (1985) 643–658.
- [45] S. Honma, T. Shirakawa, Y. Katsuno, M. Namihira, K. Honma, Circadian periods of single suprachiasmatic neurons in rats, *Neurosci. Lett.* 250 (1998) 157–160.
- [46] T. Roenneberg, M. Merrow, The network of time: understanding the molecular circadian system, *Current Biol.* 13 (2003) R198–R207.
- [47] K. Spoelstra, Dawn and dusk: behavioural and molecular complexity in circadian entrainment, Chapter 4, Ph.D. Thesis, University of Groningen, 2005.